Visible radiophotoluminescence of color centers in lithium fluoride thin films for high spatial resolution imaging detectors for hard X-rays

Maria Aurora Vincenti, Enrico Nichelatti, Valentina Nigro, Massimo Piccinini, Bruno Albertazzi, Yaniss Benkadoum, Hannibal Dabrowski, Michel Koenig, Gabriel Rigon, Paul Mabey, et al.

Visible radiophotoluminescence of color centers in lithium fluoride thin films for high spatial resolution imaging detectors for hard X-rays

Maria Aurora Vincenti [1], Enrico Nichelatti [2], Valentina Nigro [1], Massimo Piccinini [1], Bruno Albertazzi [3], Yaniss Benkadoum [3], Hannibal Dabrowski [3], Michel Koenig [3,7], Gabriel Rigon [3], Paul Mabey [4], Pascal Mercere [5], Paulo Da Silva [5], Tatiana Pikuz [6], Norimasa Ozaki [7], Evgeny Filippov [8], Sergey Makarov [8], Sergey Pikuz [8], and Rosa Maria Montereali [1,z]

[1] *ENEA C.R. Frascati, Fusion and Technologies for Nuclear Safety and Security Dept., Physical Technologies for Safety and Health Division, Photonics Micro and Nanostructures Laboratory, 00044 Frascati (RM), Italy*
[2] *ENEA C.R. Casaccia, Fusion and Technologies for Nuclear Safety and Security Dept., Physical Technologies for Safety and Health Division, Photonics Micro and Nanostructures Laboratory, Via Anguillarese 301, 00123 S. Maria di Galeria, Rome, Italy*
[3] *LULI – CNRS, CEA, Sorbonne Universités, Ecole Polytechnique, Institut Polytechnique de Paris –F-91120 Palaiseau Cedex, France*
[4] *Department of Physics, Freie Universität Berlin, Arnimallee 14, 14195 Berlin, Germany*
[5] *SOLEIL synchrotron, L'Orme des Merisiers, Départementale 128, 91190 Saint Aubin, France*
[6] *Institute for Open and Transdisciplinary Research Initiatives, Osaka University, Suita, Osaka 565-0871 Japan*
[7] *Graduate School of Engineering, Osaka University, Suita, Osaka 565-0871 Japan*
[8] *Joint Institute for High Temperature RAS, Moscov 125412, Russia*

[z] Corresponding Author rosa.montereali@enea.it

Abstract

Passive solid-state detectors based on the visible radiophotoluminescence (RPL) of stable aggregate F_2 and F_3^+ color centers in lithium fluoride (LiF) are successfully used for X-ray imaging and advanced diagnostics of intense X-rays sources. Among their advantages, these detectors offer a wide dynamic range and simplicity of use. They can be read non-destructively using a fluorescence microscope, enabling high spatial resolution over a large field of view. Optically transparent LiF films, of three different increasing thicknesses, were grown by thermal evaporation on glass and silicon substrates and subsequently irradiated with monochromatic 7 keV X-rays at several doses from 1.3×10^1 to 4.5×10^3 Gy at the SOLEIL synchrotron facility. For all the LiF films, the RPL response was found to depend linearly on the irradiation dose, with films grown on Si(100) substrates exhibiting up to a 50% higher response compared to those grown on glass. A minimum dose of 13 Gy was detected, despite the low thickness of the irradiated films. The limited thickness of the homogeneously colored LiF film allowed to obtain a spatial resolution of (0.44 ± 0.04) μm in edge-enhancement imaging experiments conducted by placing an Au mesh in front of the samples.

Introduction

Passive solid-state radiation detectors based on luminescence are widely studied and used in dosimetry[1] and imaging[2], with applications in different fields, extending from medicine to energy. In this century, the progress in photonics motivated scientific and industrial efforts devoted to research and development of novel, compact and versatile detectors based on pure and doped insulating materials containing radiation-induced point defects, whose spectral features are suitable for optical reading processes based on light excitation and detection. These types of detectors possess high intrinsic spatial resolution over a large field of view, because local radiation-induced electronic defects are utilized as minimum luminescent units, taking advantage of signal acquisition by conventional and advanced fluorescence microscopy techniques[3]. In principle, the spatial resolution is related to the atomic-scale defect dimensions, which are typically comparable to the lattice spacing and is in the range 0.4-2.0 nm for crystalline inorganic solids.

The peculiar characteristics of the visible radiophotoluminescence (RPL) of color centers (CCs) in lithium fluoride (LiF), in the form of crystals[4] and thin films[5], is gaining increased interest, especially for advancements in X-ray microscopy and microradiography at the nanoscale[6]. LiF is unique among all known materials because of its large spectral transparency and for the peculiar laser emission properties of CCs hosted in its matrix[7]. Its refractive index, ~1.39 at visible wavelengths[8], is one of the lowest for solids in natural form, and the cation-anion distance, 0.2013 nm, is the shortest among alkali halide crystals.

Versatile LiF film X-ray imaging detectors, initially proposed for soft X-rays[9], are based on the optical reading of visible RPL emitted by stable, laser-active aggregate F_2 and F_3^+ defects, which consist of two electrons bound to two and three anion vacancies, respectively. Upon light excitation in their overlapping absorption band, located at around 450 nm and known as the M band[10], they simultaneously exhibit two distinct Stokes-shifted broad emission bands, peaking at around 670 and 540 nm, respectively. Their RPL properties in optically transparent LiF films were investigated for the development of broad-band miniaturized light sources[11] in various configurations, including planar multi-layered microcavities[12].

The operation of these detectors in X-ray imaging experiments at high spatial resolution is straightforward: the investigated sample is placed in front of the LiF film surface, either in close contact or at a defined distance, depending on the source characteristics and imaging approach[6]. After exposure to X-rays, performed either in air or in vacuum depending on their energy, the impressed LiF detector is examined using a fluorescence microscope that operates in the visible range. The latent two-dimensional (2D) image stored by luminescent CCs is directly acquired by illuminating the detector with blue light, without the need for chemical development.

The RPL intensity depends linearly on the spatial concentration of aggregate CCs, which is point-by-point proportional to the X-ray intensity transmitted by the investigated sample. The thermal and optical stability of these CCs at room temperature (RT) allows for non-destructive, multiple readings of the stored X-ray images, even in daylight. The CCs information in the exposed LiF detectors is retained for years, enabling the optical reading of RPL in different laboratories. A spatial resolution of 80 nm was obtained in soft X-ray micro-radiographs stored in LiF films observed by scanning near-field optical microscopy[13]. In practice, the actual spatial

resolution is determined by the probing optical fluorescence microscope/technique used to acquire the latent images stored by CCs in LiF film after exposure to X-rays.

The simplicity of use, sub-micrometric spatial resolution and wide dynamic range make interesting application of these detectors in X-ray imaging possible with white hard X-ray beams up to 60 keV[14,15,16], even in the form of thin films combined with commercially available glass dosimeters[17]. Indeed, for ionizing radiation with depth of penetration larger than the film thickness, the resulting X-ray images exhibit a high signal-to-noise ratio, because the limited physical thickness of the luminescent thin film strongly reduces background contributions from out-of-focus planes in fluorescence images[6], thus allowing for a higher spatial resolution and contrast. The trade-off, however, is that the intensity of the collected RPL signal is lower compared to that of an entirely colored bulk crystal, due to the reduced irradiated volume, so that longer irradiation times are required and/or intense X-ray source, such as X-ray lasers, including Free Electron Lasers, were also used[18].

To increase the sensitivity of LiF film radiation detectors, it is possible to amplify the intensity of the radiated RPL by depositing the LiF film over a substrate with suitable reflective optical properties. This allows for the recovery of a fraction of the photons that would otherwise not be detected, as they would be emitted towards and lost through a transparent substrate. Among suitable substrates, Si(100) was experimentally tested with low-energy electron[19] and proton[20] beams, as well as soft X-rays[9], to obtain a substrate-enhanced RPL response of colored LiF films.

The choice of an oriented substrate plays a dominant role in the determination of the structural, and morphological properties of the as grown LiF films, which can also affect the formation, stabilization, and optical properties of CCs[21,22]. A good optical transparency of the LiF film detectors is also a critical issue for high-resolution X-ray imaging.

In this work, polycrystalline LiF films of increasing thicknesses, grown by thermal evaporation on amorphous, transparent glass and reflective silicon substrates were irradiated at several doses with a monochromatic 7 keV X-ray beam at the METROLOGIE beamline of the SOLEIL synchrotron. After irradiation, their RPL response was carefully measured using a fluorescence microscope and quantitatively studied as a function of the absorbed dose and of the film growth conditions. Edge-enhancement imaging experiments were performed at the same X-ray energy for estimating the spatial resolution of the detectors.

Experimental

Optically-transparent polycrystalline LiF films, having nominal thicknesses of 0.5, 1.1 and 1.8 μm, were grown on glass and Si(100) substrates by thermal evaporation at ENEA C.R. Frascati. The substrates were cleaned by using ultrasonic cleaning with appropriate detergents, and then fixed onto a rotating sample holder inside a cylindrical steel process chamber. The geometry of the sample holder allows obtaining LiF detectors with a circular radiation-sensitive area of diameter equal to 10 mm. The LiF powder (Merck Suprapur, 99.99% pure), placed in a tantalum crucible mounted at the base plate of the vacuum chamber below the sample-holder at a distance of 22 cm from it, was heated at about 850°C by Joule effect. The deposition of the LiF films was carried out under controlled experimental conditions with a pressure inside the vacuum chamber prior to evaporation below 1 mPa. The substrate temperature was maintained

at 300 °C using four halogen lamps controlled by a WEST N6400 single loop profile controller. The deposition rate, fixed at the nominal value of 1 nm/s, and the film thickness were monitored in situ by an INFICON XTC/2 deposition controller that employs the quartz crystal deposition monitor technique based on the piezoelectric effect.

After the deposition process, the specular reflectance and direct transmittance spectra of the LiF films were measured by a Perkin-Elmer Lambda 1050+ spectrophotometer at normal incidence (near-normal for reflectance). The spectral range was set to 190–1400 nm with a 1 nm resolution.

The LiF film detectors were irradiated at several doses (see Table 1) with a 7 keV X-ray beam at the METROLOGIE beamline of the SOLEIL synchrotron facility (Paris, France) to investigate their RPL response. The X-ray irradiations were performed by mounting the LiF film detectors on a XY motorized sample holder, which was specially designed to carry out the X-ray irradiation experiments. The X-ray beam transverse area was reduced to a square of size (2×2) mm^2 by means of two mutually perpendicular shutters. Each sample was irradiated in five distinct zones of its surface. Figure 1 shows the scheme of the experimental set-up. Using a photodiode placed in the same plane of LiF film detectors, the incident photon flux was measured before and after each irradiation. The acquired data were used to calculate the values of the irradiation doses, which are reported in Table 1.

To estimate the spatial resolution of LiF film detectors, edge-enhancement X-ray imaging experiments were carried out by placing an Au mesh (400 lines per inch, wire thickness of 12 μm) in front of them at a fixed distance of 15 mm and irradiating them with the 7 keV X-ray beam with a dose of about 4×10^3 Gy. The experimental set-up used for the imaging experiments is reported in Figure 2.

The RPL emitted by the CCs formed in the X-ray irradiated areas under blue light illumination was measured using a Nikon Eclipse 80i optical microscope operating in fluorescence mode. The microscope was equipped with a 100 W mercury lamp as excitation source and an s-CMOS camera (Andor Neo, 16 bit, cooled at -30°C) as 2D imaging detector. The excitation source was optically filtered in the blue spectral range to simultaneously excited the F_2 and F_3^+ visible RPL. The microscope software (Nikon NIS-Elements) was used for processing the acquired fluorescence images of the irradiated areas.

Results

The LiF film detectors, thermally evaporated on glass and Si(100) substrates, were characterized by spectrophotometric measurements before X-ray irradiation. Figure 3 (a) shows the specular reflectance spectra of the thickest LiF films (t = 1.8 μm) grown in the same deposition run on glass and Si(100) substrates, along with those of the bare substrates. Figure 3 (b) presents the direct transmittance spectra of the bare glass substrate and the LiF films with increasing thickness (0.5, 1.1, and 1.8 μm) thermally evaporated on glass.

Figure 4 (a) and (b) report the fluorescence images of the thickest LiF film (t = 1.8 μm) grown on glass (sample C1) and on Si(100) substrate (sample C2), respectively, irradiated with the 7 keV X-rays beam at five doses (see Table 1). In Figure 4 (a), only two of the five irradiated areas (spots) on sample C1 are clearly visible; they correspond to the highest doses listed in Table 1.

On the other hand, in Figure 4 (b), which shows the RPL areas in sample C2, three irradiated spots are clearly distinguished. In both fluorescence images, the dashed white rectangles highlight the colored spots irradiated at the lowest doses, which are not visible with the naked eye. The visible RPL intensities of all the spots, corresponding to the sample names and doses listed in Table 1, were estimated using image analysis software.

Sample	**Substrate**	**Nominal thickness (t) (μm)**	**Irradiation time**	**Dose (Gy)**
A1	glass	0.5	1m 5s	15.18 ± 0.03
			2m 5s	29.21 ± 0.09
			10m 20s	144 ± 2
			20m 35s	288 ± 1
			1h 45m	$(1.38 \pm 0.06)\times10^3$
A2	Si(100)	0.5	1m 5s	12.974 ± 0.004
			2m 5s	25.1 ± 0.2
			10m 20s	118 ± 1
			20m 35s	241 ± 5
			1h 45m	$(1.21 \pm 0.02)\times10^3$
B1	glass	1.1	1m 5s	13.80 ± 0.06
			2m 5s	26.51 ± 0.02
			10m 20s	132.7 ± 0.8
			20m 35s	262.90 ± 0.09
			1h 45m	$(1.35 \pm 0.02)\times10^3$
B2	Si(100)	1.1	1m 5s	14.76 ± 0.03
			2m 5s	28.39 ± 0.03
			10m 20s	143.6 ± 0.6
			20m 35s	283 ± 4
			1h 45m	$(1.40 \pm 0.06)\times10^3$
C1	glass	1.8	1m 5s	26.9 ± 0.5
			2m 5s	51.7 ± 0.3
			10m 20s	208 ± 9
			20m 35s	467 ± 30
			1h 45m	$(1.83 \pm 0.20)\times10^3$
C2	Si(100)	1.8	1m 5s	83.3 ± 0.3
			2m 5s	156.8 ± 0.7
			10m 20s	652 ± 25
			20m 35s	$(1.45 \pm 0.10)\times10^3$
			1h 45m	$(4.50 \pm 1.89)\times10^3$

Table 1. Irradiation times and doses absorbed by the LiF film detectors grown on glass and Si(100) substrates. The samples were irradiated with monochromatic 7 keV X-rays.

The resulting intensities are reported in Figure 5 (a) and (b) as functions of absorbed dose, along with linear best fits for each film thickness. To facilitate a clear comparison of the RPL responses of LiF detectors grown on glass and Si(100) substrates, the same scale was used for the x and y axes in both graphs. The upper x-axes also show the absorbed energy density values, based on a LiF mass density of 2.635 g/cm^3. For a quantitative analysis, Table 2 presents the slopes of the best-fit straight lines in Figure 5 (a) and (b), as well as the ratios of the slopes for the films grown on Si(100) to those on glass in the same deposition runs.

LiF film sample	**Substrate**	**t** (μm)	**Slope (10^{-2})**	**Slope/t (10^{-2}/μm)**	**Si/glass slope ratio**
A2	Si(100)	0.5	1.3±0.1	2.6±0.2	1.6±0.3
A1	glass		0.8±0.1	1.6±0.2	
B2	Si(100)	1.1	3.0±0.3	2.7±0.3	1.5±0.2
B1	glass		2.0±0.1	1.82±0.09	
C2	Si(100)	1.8	3.7±0.1	2.06±0.06	1.5±0.2
C1	glass		2.4±0.2	1.3±0.1	

Table 2. Slopes of the best-fit straight lines reported in Figure 5 (a) and (b), ratios of the slopes to the film thicknesses, and ratios of the slopes for the films grown on Si(100) to those on glass in the same deposition run.

The edge enhancement X-ray experiment involved acquiring the fluorescence image of the Au mesh stored in the 1.8 μm thick LiF film grown on glass irradiated at a dose of 3.84×10^3 Gy. The image was acquired at low magnification (Figure 6 (a)) and high magnification (Figure 6 (b)) to test the imaging capabilities of LiF film X-ray detectors and evaluate their spatial resolution. Figure 6 (c) reports the RPL intensity profile measured along the white line drawn in Figure 6 (b). Figure 6 (d) shows the RPL intensity profile of a left portion (from 52 to 60 μm) of the second fluorescent spot of Figure 6 (c), together with the Gaussian best fit (dashed line) of the highest peak of the diffraction pattern. Similar patterns were obtained for the LiF film grown on Si(100).

Discussion

As shown in Figure 3 (a), the reflectance spectrum of the LiF film grown on Si(100) is higher than that of the LiF film grown on glass. This effect is ascribed to the optical reflectivity of the bare substrates in the visible spectral range, where both the excitation blue light and the broad RPL emission bands of the aggregate F_2 and F_3^+ defects are located. In Figure 3(b), the

transmittance spectra of the LiF films thermally evaporated on glass are shown. For the thickest film, a decrease of the measured transmittance is observed, especially towards the short wavelengths. This could be attributed to volume scattering caused by poorer film homogeneity, potentially due to increased grain interstitials compared to the other two films. Indeed, being a form of Rayleigh scattering, the intensity of volume scattering is inversely proportional to λ^4. Further investigations are underway to gain a better understanding this difference.

The X-ray depth of attenuation at the energy of 7 keV is estimated to be 220 μm[23], which is much higher than the thickness of the investigated samples. This means that the coloration of the LiF films can be assumed to be homogeneous. For this reason, the observed differences in the spot intensities in the fluorescence images in Figure 4 (b) with respect to Figure 4 (a) are essentially ascribed to the higher reflectance of the silicon substrate in the visible spectral range.

Higher RPL signals on colored LiF films directly grown on Si(100) were detected for all doses and thickness, as one can see by comparing Figures 5 (a) and (b). Additionally, it was found that the RPL intensities depend linearly on the irradiation dose in all the investigated dose range for LiF film detectors grown on both glass and Si(100) substrates for all the film thicknesses. As the spectrally integrated RPL signal is due to both aggregate F_2 and F_3^+ active defects hosted in polycrystalline matrices, this behavior is particularly interesting for radiation imaging and dosimetry.

For a quantitative comparison of the film sensitivity, the slopes of the best-fitting straight lines in Figure 5 (a) and (b), reported in Table 2, are higher for LiF films grown on Si(100) substrate with respect to glass for all the film thicknesses. Table 2 also reports the values of the ratios of the slopes of LiF films grown on Si(100) to those grown on glass in the same deposition run, which is about 1.5 for all three thicknesses. This ratio corresponds to an enhancement of about 50% of the RPL signal, ascribable to the reflectivity of the silicon substrate in the visible spectral range, where the emission bands of the F_2 and F_3^+ CCs are located[24].

The lowest detected dose, delivered to the thinnest (t = 0.5 μm) LiF film detector grown on Si(100), was of about 13 Gy (34 mJ/cm^3), despite the small thickness of the radiation-sensitive LiF film. This value is comparable with the minimum of 10 Gy reported for a LiF film[17] about 1 μm thick grown on an Ag-doped glass dosimeter and irradiated by an X-ray tube equipped with a copper target, whose broad X-ray spectrum is peaked at about 8 keV.

Increasing the film thickness, an increase in the RPL signal is expected. The slopes reported in Table 2 for the A and B samples are directly proportional to the film thickness. Moving from the thinnest 0.5 um thick film to the one of thickness 1.1 um, the RPL signal is more than doubled within the experimental errors. At the highest thickness of 1.8 um, a thickness 60% larger than the 1.1 μm thickness of the B samples, an increase of only 20% is observed for both types of substrate, possibly relatable to the lowest transmittance measured in Figure 4 (b). Further experiments are under way to investigate this behavior and improve the optical transparency of thicker films.

From the Gaussian best fit (dashed line) of the highest peak of the diffraction pattern in Figure 6 (d), a Half Width at Half Maximum of the Gaussian function equal to (0.44 ± 0.04) μm was obtained. This value is comparable with the optical microscope diffraction limited resolution, and it is similar to that obtained in the diffraction pattern recorded at the same X-ray energy on the LiF film grown on Si (100) [25]. This confirms that the submicrometric spatial resolution of

LiF film detectors, even with high-penetrating radiation, is a peculiarity of these detectors based on RPL, independently from the selected substrate.

Conclusions

The visible RPL response of optically transparent polycrystalline LiF thin films of increasing thicknesses, deposited by thermal evaporation on glass and Si(100) substrates in controlled experimental conditions and irradiated with monochromatic 7 keV X-rays at different doses, was measured using a fluorescence microscope and tested in edge-enhancement imaging experiments.

A linear behavior as a function of the absorbed dose in the range between 13 and 4.5×10^3 Gy was found both for LiF films grown on glass and Si(100) substrate for all the investigated thickness. A substrate-enhanced RPL response amplified by 50% was obtained for LiF film detectors grown on Si(100) with respect to those deposited on glass in the same deposition run. This is ascribed to the high reflectivity of the silicon substrate at the visible wavelengths, where the absorption and emission bands of aggregate CCs are located.

A high submicrometric (< 0.5 μm) spatial resolution, limited only by the diffraction of the optical microscope, was obtained on a large field of view (> 1 cm^2). The lowest dose of 13 Gy was successfully detected by means of the thinnest LiF film grown on Si(100) substrate, only 0.5 μm thick, encouraging the investigation of LiF film detectors as 2D imaging dosimeters. Further experiments with monochromatic X-rays at energies of several keV are under way to study the LiF film sensitivity and their RPL dose response, and improve the reproducibility of the observed behavior by a careful control of the film growth conditions.

Acknowledgments

Many thanks are due to S. Libera for his skillful technical assistance. This research has been carried out within the TECHEA (Technologies for Health) Project, funded by the Italian National Agency for New Technologies, Energy and Sustainable Economic Development (ENEA), Italy and partly supported by KAKENHI (grant no. 21K03499) from the Japan Society for the Promotion of Science (JSPS). JIHT RAS team was supported by MSHE RF (grant No. 075-15-2021-1352).

References

1. K. Maesh, P. S. Weng, C. Furetta, *Thermoluminescence in solids and its applications*, NTP, England, UK (1989).
2. N. Itoh, M. Stoneham, *Materials Modification by Electronic Excitation*, Cambridge University Press, Cambridge, UK (2001).
3. S. K. Sekatskii, V. S. Letokhov, *Appl Phys B,* **63**, 525 (1996).
4. J. H. Schulman, R. J. Ginther, and C. C. Klick, R. S. Alger and R. A. Levy, *J. Appl. Phys.,* **22**, 12 (1951) 1479.
5. R. M. Montereali, in *Handbook of Thin Film Materials*, H. S. Nalwa, Editor, Vol.3: Ferroelectric and Dielectric Thin Films, Ch.7, p. 399, Academic Press, S. Diego (2002).
6. R. M. Montereali, F. Bonfigli, E. Nichelatti, M. Piccinini, M. A. Vincenti, in *Optical NanoSpectroscopy*, A. J. Meixner, M. Fleischer, D. P. Kern, E. Sheremet and N. McMillan,

Editors, Vol. 3: Applications, p. 69, De Gruyter, Berlin, Boston (2023).
7. T. T. Basiev, S. B. Mirov, V. V. Osiko, *IEEE J. Quantum Electron.,* **24**, 1052 (1988).
8. E. D. Palik, W. R. Hunter, in *Handbook of Optical Constants of Solids*; E. D. Palik, Editor, Vol. 1, p. 675, Academic Press, San Diego, California, USA (1985).
9. G. Baldacchini, F. Bonfigli, A. Faenov, F. Flora, R. M. Montereali, A. Pace, T. Pikuz, L. Reale, *J. Nanosci. Nanotechno.,* **3**, 483 (2003).
10. J. Nahum, D. A. Wiegand, *Phys. Rev.,* **154**, 817 (1967).
11. R. M. Montereali, in *Spectroscopy of Systems with Spatially Confined Structures*, B. Di Bartolo, Editor, p. 617, NATO Science Series, Kluwer Academic Publisher, (2003).
12. F. Bonfigli, B. Jacquier, F. Menchini, R. M. Montereali, P. Moretti, E. Nichelatti, M. Piccinini, H. Rigneault, F. Somma, in *Spectroscopy of Systems with Spatially Confined Structures*, B. Di Bartolo, Editor, p. 697, NATO Science Series, Kluwer Academic Publisher, (2003).
13. A. Ustione, A. Cricenti, F. Bonfigli, F. Flora, A. Lai, T. Marolo, R. M. Montereali, G. Baldacchini, A. Faenov, T. Pikuz and L. Reale, *Jpn. J. Appl. Phys*., **45**, 2116 (2006).
14. S. Almaviva, F. Bonfigli, I. Franzini, A. Lai, R. M. Montereali, D. Pelliccia, A. Cedola, S. Lagomarsino, *Appl. Phys. Lett.*, **89,** 54102 (2006).
15. F. Bonfigli, A. Cecilia, S. Heidari Bateni, E. Nichelatti, D. Pelliccia, F. Somma, P. Vagovic, M. A. Vincenti, T. Baumbach and R. M. Montereali, *Rad. Meas.*, **56,** 277 (2013).
16. E. Nichelatti, F. Bonfigli, M.A. Vincenti, A. Cecilia, P. Vagovic, T. Baumbach, R. M. Montereali, *Nucl. Instr. Meth. A,* **833**, 68 (2016).
17. T. Kurobori and A. Matoba, *Jpn. J. Appl. Phys*., **53**, 14 (2014).
18. T. A. Pikuz, A. Ya. Faenov, Y. Fukuda, M. Kando, P. Bolton, A. Mitrofanov, A. V. Vinogradov, M. Nagasono, H. Ohashi, M. Yabashi, K. Tono, Y. Senba, T. Togashi and T. Ishikawa, *Applied Optics,* **52**, 3, 509 (2013).
19. G. Baldacchini, E. Burattini, L. Fornarini, A. Mancini, S. Martelli, R. M. Montereali, *Thin Solid Films,* **330**, 67 (1998).
20. M. Leoncini, M. A. Vincenti, F. Bonfigli, S. Libera, E. Nichelatti, M. Piccinini, A. Ampollini, L. Picardi, C. Ronsivalle, A. Mancini, A. Rufoloni, R. M. Montereali, *Opt. Mater.*, **88,** 580 (2019).
21. R. M. Montereali, A. Mancini, S. Martelli, F. Menchini, P. Picozzi, *Appl. Organometal. Chem.,* **15**, 407 (2001).
22. R. M. Montereali and A. P. Voitovich, in *Nano-Optics: Principles Enabling Basic Research and Applications*, B. Di Bartolo, J. Collins, L. Silvestri, Editors, p.149 NATO Science for Peace and Security Series B: Physics and Biophysics, Springer, Dordrecht, (2017).
23. http://henke.lbl.gov/optical_constants/atten2.html.
24. M.A. Vincenti, M. Leoncini, S. Libera, A. Ampollini, A. Mancini, E. Nichelatti, V. Nigro, L. Picardi, M. Piccinini, C. Ronsivalle, A. Rufoloni, R.M. Montereali, *Opt. Mater.,* **119**, 111376 (2021).
25. M.A. Vincenti, R.M. Montereali, E. Nichelatti, V. Nigro, M. Piccinini, M. Koenig, P. Mabey, G. Rigon, H.J. Dabrowski, Y. Benkadoum, P. Mercere, P. Da Silva, T. Pikuz, N. Ozaki, S. Makarov, S. Pikuz and B. Albertazzi, *J. Inst.*, **18**, C04012 (2023).

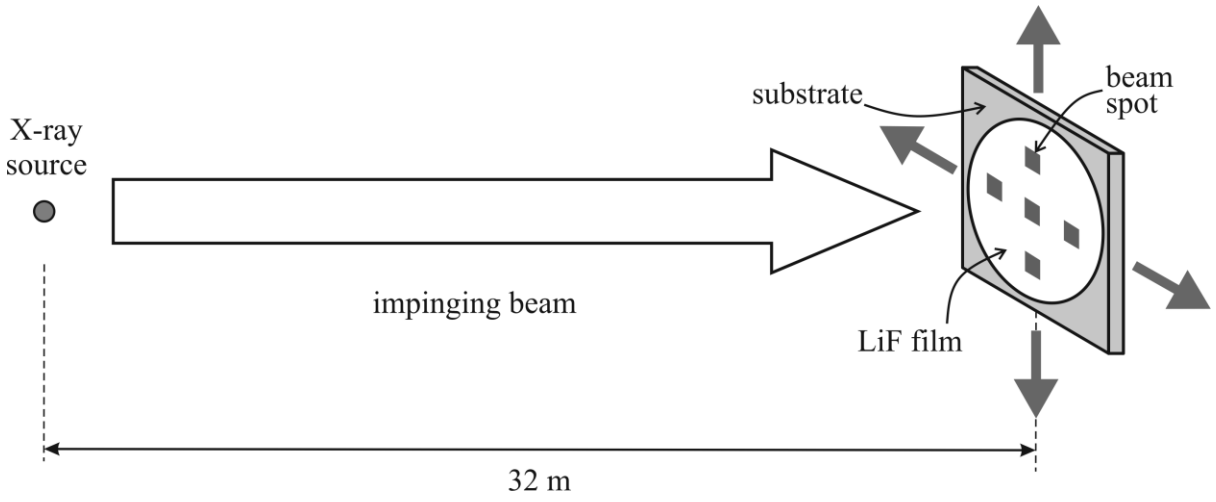

Figure 1. Scheme of the experimental set-up used to irradiate LiF film detectors in five zones of their surface each corresponding to a different dose value, with a 7 keV X-ray beam at the METROLOGIE beamline of the SOLEIL synchrotron facility. The four arrows drawn at the LiF detector indicate that it is mounted on a XY motorized sample holder.

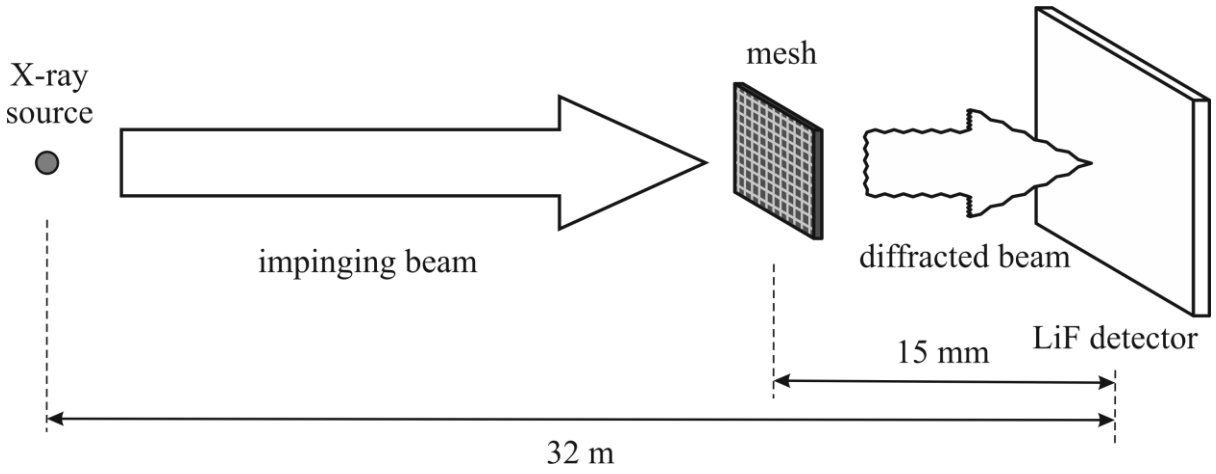

Figure 2. Scheme of the experimental set-up used to perform edge-enhancement X-ray imaging experiments at the METROLOGIE beamline of the SOLEIL synchrotron facility.

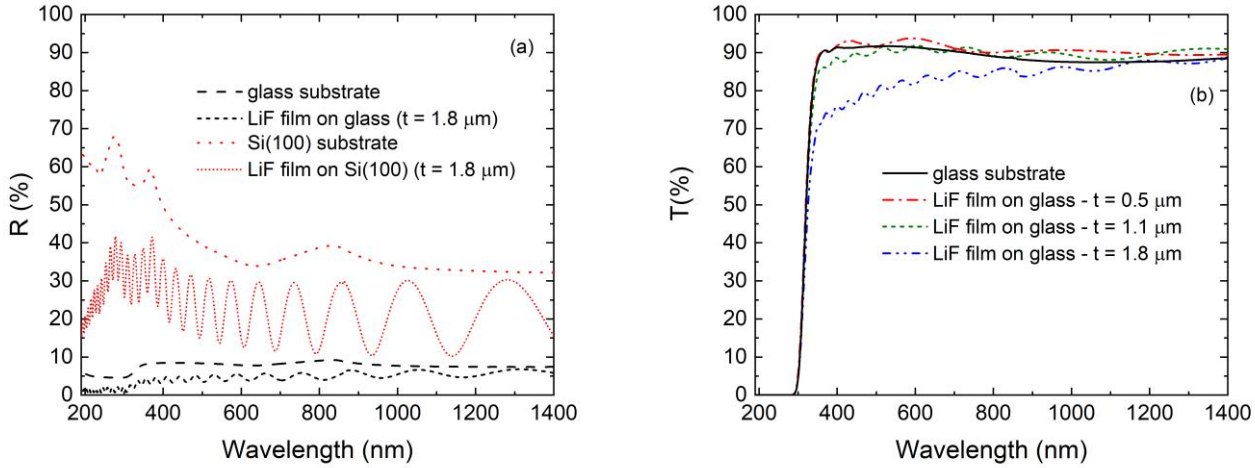

Figure 3. (a) Specular reflectance, *R*, spectra of the thickest LiF films (t = 1.8 μm) grown in the same deposition run on glass and Si(100) substrates, along with those of the bare substrates; (b) direct transmittance, *T*, spectra of the bare glass substrate and of the LiF films of increasing thickness grown on glass.

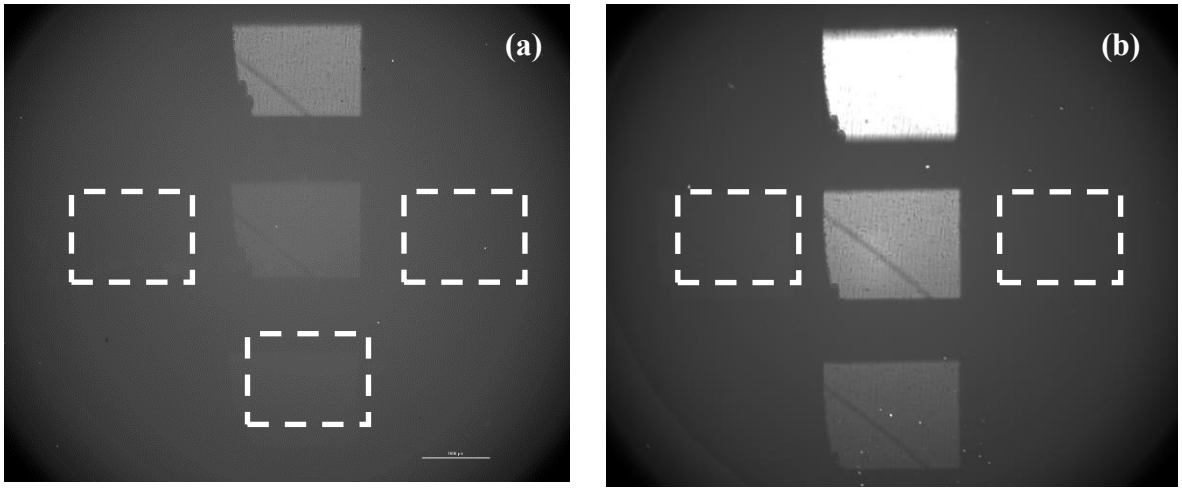

Figure 4. Fluorescence images of the thickest LiF films (t = 1.8 μm) grown on glass (a) and Si(100) (b) substrates irradiated with monochromatic 7 keV X-rays at five doses. Image field sizes of (1.67×1.41) cm^2 (bar size = 1 mm). The dashed white rectangles highlight the lowest-dose irradiated spots, which are not visible with the naked eye.

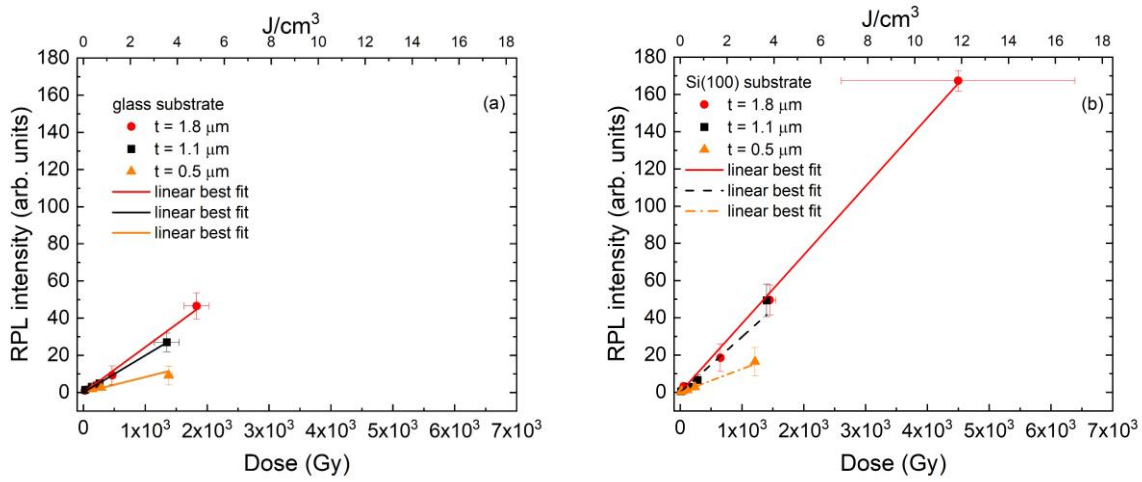

Figure 5. RPL response vs. dose of LiF film detectors grown on glass (a) and Si(100) (b) substrates irradiated with monochromatic 7 keV X-rays, together with their linear best fit for each film thickness (0.5, 1.1 and 1.8 µm). To facilitate a clear comparison of the RPL responses of LiF detectors grown on glass and Si(100) substrates, the same scale was used for the x and y axes in both graphs.

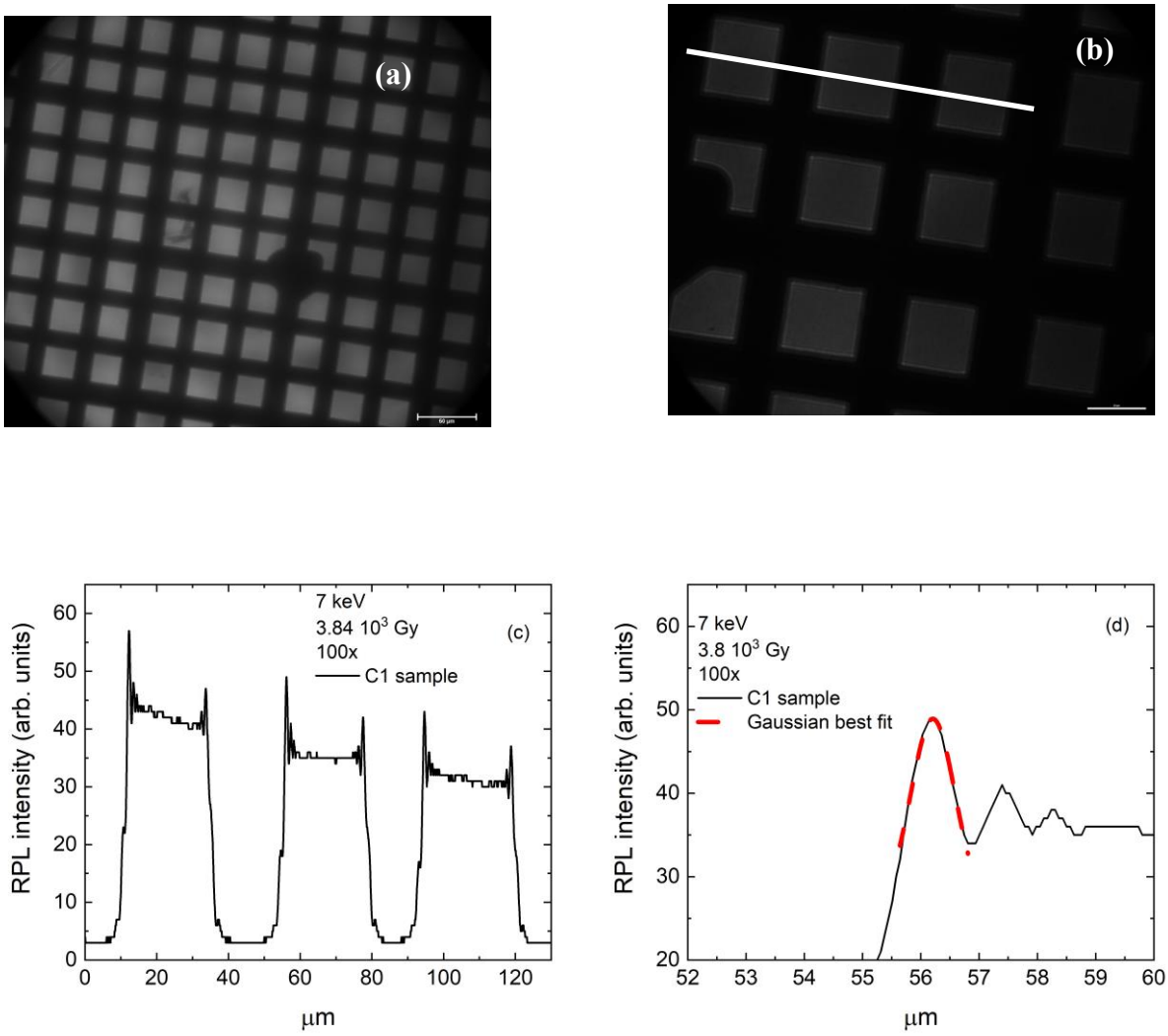

Figure 6. (a) Fluorescence image of the Au mesh stored in the 1.8 μm thick LiF film grown on glass irradiated with 7 keV X-rays at a dose of 3.84×10^3 Gy. The image was acquired using an objective magnification of 40× (bar size = 50 μm) and (b) 100× (bar size = 20 μm); (c) RPL intensity profile measured along the white line in Figure 6 (b); (d) RPL intensity profile of a left portion (from 52 to 60 μm) of the second fluorescent spot in Figure 6 (c) together with the Gaussian best fit (dashed line) of the highest peak of the diffraction pattern.